Available online at www.sciencedirect.com
ScienceDirect
Sedimentary Geology 191 (2006) 67–87
Sedimentary Geology
www.elsevier.com/locate/sedgeo

Sedimentology of rift climax deep water systems; Lower Rudeis Formation, Hammam Faraun Fault Block, Suez Rift, Egypt

Christopher W. Leppard *, Rob L. Gawthorpe

Basin and Stratigraphic Studies Group, School of Earth, Atmospheric and Environmental Sciences (SEAES), University of Manchester, Oxford Road, Manchester, M13 9PL, UK

Received 1 February 2005; received in revised form 11 January 2006; accepted 19 January 2006

Abstract

In most marine rift basins, subsidence outpaces sedimentation during rift climax times. Typically this results in sediment-starved hangingwall depocentres dominated by deep-marine mudstones, with subordinate local development of coarser clastics in the immediate hangingwall derived from restricted catchments on the immediate footwall scarp. To highlight the spatial variability of rift climax facies and the controls upon them, we have investigated the detailed three-dimensional geometry and facies relationships of the extremely well exposed Miocene, rift climax Lower Rudeis Formation in the immediate hangingwall to the Thal Fault Zone, Suez Rift, Egypt. Detailed sedimentological analyses allows the Lower Rudeis Formation to be divided into two contemporaneous depositional systems, (1) a laterally continuous slope system comprising, hangingwall restricted (<250 m wide) slope apron, slope slumps, fault scarp degradation complex and laterally extensive lower slope-to-basinal siltstones, and (2) a localized submarine fan complex up to 1 km wide and extending at least 2 km basinward of the fault zone.

Interpretation of individual facies, facies relationships and their spatial variability indicate that deposition in the immediate hangingwall to the Thal Fault occurred via a range of submarine concentrated density flows, surge-like turbidity flows, mass wasting and hemipelagic processes. Major controls on the spatial variability and stratigraphic architecture of the depositional systems identified reflect the influence of the steep footwall physiography, accommodation and drainage evolution associated with the growth of the Thal Fault. The under-filled nature of the hangingwall depocentre combined with the steep footwall gradient result in a steep fault-controlled basin margin characterised by either slope bypass or erosion, with limited coastal plain or shelf area. Sediment supply to the slope apron deposits is controlled in part by the evolution and size of small footwall drainage catchments. In contrast, the localized submarine fan is interpreted to have been fed by a larger, antecedent drainage network. The structural style of the immediate footwall is also believed to exert a control on facies development and stratigraphic evolution. In particular, fault scarp degradation is enhanced by fault propagation folding which creates basinward-dipping bedding planes in the pre-rift footwall strata that large pre-rift blocks slide on.

Keywords: Deep marine; Gulf of Suez; Miocene; Rift; Turbidite

1. Introduction

Rift climax deposits in marine rift basins are typically characterised by deep marine, mudstone-dominated facies (Prosser, 1993) due to sedimentation being

* Corresponding author. Present address: Norsk Hydro Research Centre, Sandsliveien 90, 5020 Bergen, Norway. Tel.: +47 55992519; fax: +47 55995704.
E-mail address: Chris.Leppard@Hydro.com (C.W. Leppard).

0037-0738/$ - see front matter © 2006 Elsevier B.V. All rights reserved.
doi:10.1016/j.sedgeo.2006.01.006

outpaced by subsidence. Typically this creates deepwater (in excess of several 100 m), sediment-starved, hangingwall depocentres. These are filled with locally restricted, footwall-derived coarse clastics, axial turbidites and basinal hemipelagic deposits (Gawthorpe and Hurst, 1993; Prosser, 1993; Gawthorpe et al., 1994; Gawthorpe and Leeder, 2000; McLeod et al., 2002). These facies are deposited when the rate of displacement on the bounding fault is at a maximum, and have been identified in many modern and ancient rift basins (e.g. Gulf of Corinth (Gawthorpe and Leeder, 2000), North Sea (Prosser, 1993; McLeod et al., 2002), and East Greenland rift (Surlyk, 1989; Seidler et al., 2004)). Controls on the spatial distribution of rift climax facies have been highlighted as a complex interaction between the evolution and linkage of normal fault populations, the evolution of drainage networks and catchments, bedrock lithology, and variations in sea/lake level (Gawthorpe and Leeder, 2000; Gawthorpe et al., 2003). Numerical models of normal fault populations have confirmed the close relationship between evolving fault population and the gross stratigraphic architecture of syn-rift deposits (Cowie et al., 2000). However, the detailed temporal and spatial distribution of facies and stratal geometries has not been documented in detail, particularly in the context of a well-constrained fault growth history.

To date, few studies have focused on documenting the detailed three-dimensional characteristics of facies and stratigraphic architecture of coarse-grained rift climax deposits in the hangingwall to a basin-bounding normal fault zone (e.g. East Greenland rift, Surlyk, 1989). Subsurface seismic data sets are unable to offer the vertical resolution and, even with well penetration, the continuous three-dimensional sedimentological data required to document facies relationships and stratigraphic architecture are not available in such data sets. This paper is able to address the issues stated by focusing on the rift climax, deep marine, Miocene, Lower Rudeis Formation in the immediate hangingwall to the Thal border fault zone to the Hammam Faraun Fault Block, Suez Rift, Egypt (Fig. 1). The excellent exposure on this uplifted rift shoulder allows the tracing of facies over distances of several kilometres, approximately the same spatial scale as the depositional systems, in both fault parallel and fault perpendicular sections. Well-constrained structural studies of the Hammam Faraun Fault Block and its structural evolution (e.g. Moustafa and Abdeen, 1992; Moustafa, 1996a; Gawthorpe et al., 2003) allow the observed facies variations to be placed within a tightly constrained structural framework. The development of a

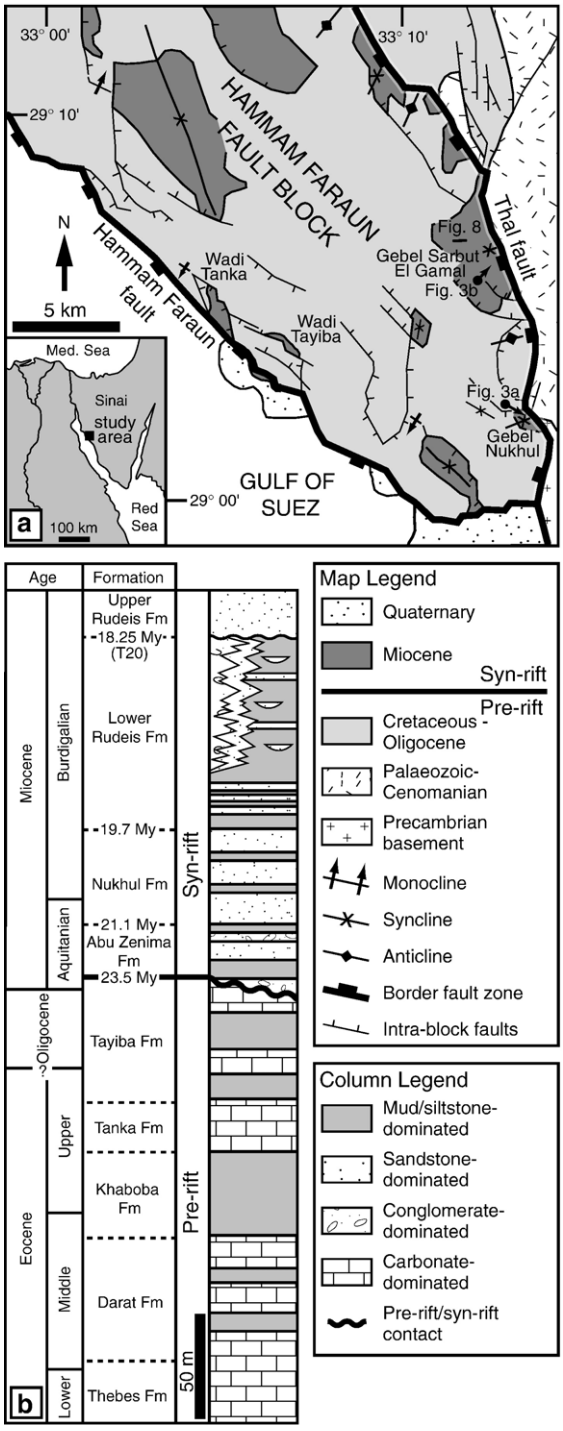

Fig. 1. (a) Simplified geological map of the Hammam Faraun Fault Block (modified from Moustafa, 1993). Inset shows the regional geographical setting. (b) Simplified stratigraphy of the study area. The interval of interest is the syn-rift Lower Rudeis Formation. Stratigraphic ages are based on magnetostratigraphy (Bentham et al., 1996) and biostratigraphy (Krebs et al., 1997).

process-based facies model for the Lower Rudeis Formation allows the controls on sediment distribution and stratigraphic evolution during rift climax times to be identified.

2. Geological setting

The Gulf of Suez is a failed intracontinental rift that forms the NW–SE-trending continuation of the Red Sea rift system (Fig. 1a), and was initiated during the late Oligocene to early Miocene by the NE–SW separation of the African and Arabian plates (Colletta et al., 1988; Patton et al., 1994). The rift is up to 80 km wide and 300 km long, and comprises a series of classic half-graben tilted fault blocks, typically <20 km wide and up to 50 km long (Colletta et al., 1988; Patton et al., 1994). The dip polarity of the fault blocks and their bounding faults changes along the length of the rift, dividing the rift into three distinct dip provinces separated by major accommodation zones (Bosworth, 1985; Patton et al., 1994; Moustafa, 1996b).

The Hammam Faraun fault block is one of the main fault blocks in the central dip province of the Suez rift and is exposed on the western side of the Sinai Peninsula (e.g. Moustafa and Abdeen, 1992; Patton et al., 1994; Moustafa, 1996a; Fig. 1a). The fault block has a half-graben geometry, dipping moderately to the east (12–15°), is up to 25 km wide and 40 km long, and is bounded to the east and west by major, down-to-the-west normal fault zones, the Thal and Hammam Faraun fault zones respectively (Moustafa and Abdeen, 1992; Moustafa, 1996a; Sharp et al., 2000a; Fig. 1a). These major border fault zones are segmented, having a zig-zag pattern in plan view, and dip steeply (60–80°) to the SW, with a maximum displacement of 2–5 km. Internally, the fault block is dissected by several short (4–10 km), low displacement (<1 km) fault segments that are interpreted to have evolved by linkage of initially isolated segments (Sharp et al., 2000b; Jackson et al., 2002; Gawthorpe et al., 2003). Deformation became progressively localized during rifting onto the major block-bounding faults that define the present-day structure of the rift (Gupta et al., 1998; Sharp et al., 2000b; Gawthorpe et al., 2003).

Late pre-rift strata of the Hammam Faraun fault block is ca. 375 m thick and predominantly comprised of Lower to Upper Eocene age carbonates that are interpreted to have been sub-horizontal prior to extension (e.g. Moustafa and Abdeen, 1992; Moustafa, 1996a; Sharp et al., 2000b). Overall, the late pre-rift displays a shallowing-upwards Eocene succession of cherty micritic wakestone slope deposits of the Thebes Formation to carbonate platform deposits of the Tanka Formation (Abul-Nasr and Thunell, 1987; Abul-Nasr, 1992). A biostratigraphically defined unconformity separates the Eocene succession from the Lower Oligocene, low-energy shelf to offshore deposits of the late pre-rift Tayiba Formation (Abul-Nasr, 1990; Refaat and Imam, 1999; Jackson et al., 2005).

In the immediate hangingwall to the Thal border fault zone (Fig. 1a) fluvial deposits of the rift-initiation, Abu Zenima Formation (24–21.5 Ma) generally overly the pre-rift/syn-rift unconformity (23.5 Ma) and are characterised by a sheet-to-channel-like, flood-generated, cobble conglomerates interbedded with medium-grained fluvial sandstones and floodplain mudstones. The top of this fluvial succession is marked by a widespread major marine transgression, and deposition of the shallow marine-to-offshore deposits of the Nukhul Formation (21.5–19.7 Ma), comprising a series of shoaling upwards packages of offshore mudstones capped by shoreface sandstones. The Abu Zenima and Nukhul Formations are interpreted to have been deposited in fluvial to shallow marine environments during a slow subsidence rift-initiation phase where sedimentation kept pace with subsidence (Gawthorpe et al., 2003).

Overlying the Nukhul Formation are deep marine deposits of the rift climax Lower Rudeis Formation. The Lower Rudeis Formation (19.7–18.25 Ma), the subject of this paper, is characterised by locally restricted, footwall-derived coarse clastic, submarine fan and slope apron complexes and hemipelagic deposits interpreted to have been deposited during a rapid subsidence rift climax phase (e.g. Garfunkel and Bartov, 1977; Patton et al., 1994; Krebs et al., 1997; Gawthorpe et al., 2003). The transition from the Lower to Upper Rudeis Formations is marked by the mid-Clysmic or mid-Rudeis unconformity (T20 ca.18.25 Ma; Krebs et al., 1997) that is believed to be associated with a regional tectonic event (Garfunkel and Bartov, 1977; Wescott et al., 1996; Krebs et al., 1997). Sedimentation during the Upper Rudeis is characterised by fan deltas along the rift margins, submarine fans in hangingwall depocentres, and hangingwall shorelines (e.g. Smale et al., 1988; Evans, 1988).

3. Sedimentology

Detailed sedimentological analysis of the Lower Rudeis Formation is based on: logged sections, field mapping, horizontal facies variations, correlating key surfaces and field-based interpretation on large-format photo panoramas. These analyses suggest deposition in

Table 1
Summary of the sedimentary facies

Facies association		Facies	Geometry	Description	Process
Slope deposits	Slope apron (A)	Lobate medium to coarse-grained bedded sandstone (A1)	Broad lobe, strike <500 m, dip <250 m, bed thickness 5–6 m	Medium to coarse-grained, poorly sorted, bioclastic sandstone. Bedded on 10 cm scale with gradational basal contact and sharp top. Bioclasts (shell hash) and lithoclasts (30 mm to 60 cm diameter) present throughout.	Concentrated density flow
		Lobate cobble-grade conglomerate (A2)	Lobate, strike <400 m, dip <150 m, bed thickness 2–5 m	Cobble-grade, moderately sorted, clast-supported conglomerate. Forms fining upwards packages 2 to 5 m thick with a sharp base and gradational top. Lithoclasts composed of re-worked pre-rift limestone and chert.	Concentrated density flow
	Slumps and slides (B)	Contorted medium to coarse-grained bedded sandstone (B1)	Slump sheet, strike <400 m, dip <300 m, bed thickness 2–5 m	Medium to coarse-grained, poorly sorted, bioclastic sandstone. Displays contorted bedding and a sharp basal contact (slide plane). Bioclasts (shell hash) and lithoclasts (30 mm to 60 cm diameter) present throughout.	Slumping and sliding
	Fault scarp degradation (C)	Sub-angular mega-breccia (C1)	Elongate apron, strike >2 km, dip <250 m, bed thickness up to 150 m	Pebble to boulder-grade, sub-angular, cast-supported breccia. Average clast size 45 cm up to >200 m, composed of predominantly re-worked pre-rift limestone of the Thebes Fm.	Rock fall
	Lower slope (D)	Green laminated siltstone (D1)	Extensive sheet, strike >5 km, dip >2 km, bed thickness 20–50 mm	Green laminated siltstone, bedded on 20 mm to 50 mm scale. Basal contact sharp, locally deformed, displaying tight isoclinal folds and thrusts.	Hemipelagic
		Siltstone to fine-grained sandstones (D2)	Sheet, strike >500 m, dip >500 m, bed thickness 20–100 mm	Siltstone to fine-grained thinly laminated sandstone. Bedded on a 2 to 10 cm scale with a sharp contact with adjacent beds. Sedimentary structures present include current ripples and planar lamination.	Surge-like turbidity flow
Submarine fan complex	Proximal fan (E)	Cobble-grade conglomerate (E1)	Lobate wedge, strike <1 km, dip <250 m, bed thickness 5–6 m	Cobble-grade, moderately sorted, sub-angular to rounded conglomerate composed of pre-rift limestone and chert clasts 10 to 15 cm diameter, form fining upwards packages with a sharp base and gradational top.	Concentrated density flow
		Medium to coarse-grained bedded sandstone (E2)	Lobate wedge, strike <1 km, dip <250 m, bed thickness 5–6 m	Medium to coarse-grained, poorly sorted, bioclastic sandstone. Bedded on a 15 cm scale with a sharp base and top. Bioclasts (shell hash, oysters) and lithoclasts (limestone, chert) up to 3 cm diameter present throughout.	Concentrated density flow
		Coarse-grained massive sandstone (E3)	Lens/channel, strike <100 m, dip <600 m, bed thickness 1–2 m	Coarse-grained, poorly sorted, massive bioclastic sandstone. Erosive base with sub-angular limestone and chert conglomerate lag with rare outsized clasts up to 3 cm diameter, bioclasts include shell hash and algal rhodoliths.	Concentrated density flow
	Mid fan (F)	Pebble-grade conglomerate (F1)	Sheet/broad lobe, strike <500 m, dip <800 m, bed thickness 1–2 m	Pebble-grade, moderately sorted, sub-angular to rounded conglomerate. Fining upwards packages composed of reefal debris, pre-rift limestone and chert. Sharp basal contact and gradational top.	(Transitional) Concentrated density flow

Table 1 (*continued*)

Facies association		Facies	Geometry	Description	Process
Submarine fan complex		Medium to coarse-grained upward thickening sandstone (F2)	Sheet/broad lobe, strike <1 km, dip <1 km, bed thickness 1–5 m	Medium to coarse-grained, poorly sorted, bioclastic sandstone. Bedding thickness increases up through the unit with low angle beds and m scale trough cross-bedding. Basal and top contacts typically sharp. Lithoclasts up to 15 cm diameter (limestone and chert) and bioclasts (reefal debris and shell hash) present throughout.	(Transitional) Concentrated density flow
		Coarse-grained massive sandstone (F3)	Sheet/lens, strike <500 m, dip <1 km, Bed thickness 2–4 m	Coarse-grained, poorly sorted, massive sandstone. Sharp basal contact and flat topped, rare outsized lithoclasts up to 10 cm and bioclasts (shell hash) present throughout.	(Transitional) Concentrated density flow
	Distal fan (G)	Coarse-grained channelised sandstone (G1)	Channelised, strike <30 m, dip <1.5 km, bed thickness up to 5 m	Medium to granule-grade, poorly sorted, bioclastic sandstone. Erosive stacked channelised geometry with a sharp top, lithoclasts (limestone and chert) and bioclasts (reefal debris, shell hash) present throughout.	(Transitional) Concentrated density flow
		Fine medium-grained sheet sandstone (G2)	Sheet, strike >250 m, dip >200 m, bed thickness up to 3 m	Fine to medium-grained, bioclastic sandstone. Nodular cementation displays crude bedding on a 30 cm scale. Sharp slightly erosive base with planar top. Rare lithoclasts (limestone and chert) up to 2 cm diameter and bioclasts (shell hash, corals) present throughout.	Surge-like turbidity flow
		Siltstone to fine-grained sandstone (G3)	Sheet, strike >500 m, dip >500 m, bed thickness 20–150 mm	Siltstone to fine-grained laminated sandstone. Contacts with adjacent beds typically sharp, sedimentary structures present include planar lamination and current ripples with rare 2 mm diameter mudstone rip-up clasts.	Surge-like turbidity flow

two broadly contemporaneous depositional systems in the hangingwall to the Thal fault zone, a laterally continuous slope system and a localized submarine fan complex (Table 1). Deposits of the slope system comprise four facies associations: (A) slope apron, (B) slumps and slides, (C) fault scarp degradation complex, and (D) lower slope. The submarine fan complex comprises three facies associations: (E) proximal fan, (F) mid fan and (G) distal fan.

3.1. Slope system

The slope apron, fault scarp degradation complex and slumps and slides occur as a narrow (<250 m) wide facies belt in the immediate hangingwall of the Thal Fault and pass into the lower slope deposits. The four facies associations of the slope depositional system are laterally extensive parallel to the Thal Fault.

3.1.1. Facies Association A: slope apron

Facies Association A consists of two facies that form a laterally continuous coarse-grained sandstone (A1) (70%) and conglomerate (A2) (30%) apron in the immediate hangingwall to the Thal fault zone. This apron is at least 200 m thick with a strike extent of >3 km and pinches-out basinwards over <250 m. The apron is comprised of a stacked succession of basinward-tapering wedges with a lateral continuity of <500 m along strike that display a lobate geometry in a fault-parallel section.

Lobate medium to coarse-grained bedded sandstone (A1) consists of poorly sorted, pale brown, bioclastic sandstones that form 5 to 6 m thick sheets or broad lobes that are up to 500 m wide. Internally Facies A1 consists of decimetre-scale beds that are often disturbed by large (ca. 0.5 m) sub-angular, out-sized limestone lithoclasts (Fig. 2a, b). Pre-rift derived limestone and chert lithoclasts up to 30 mm diameter are present

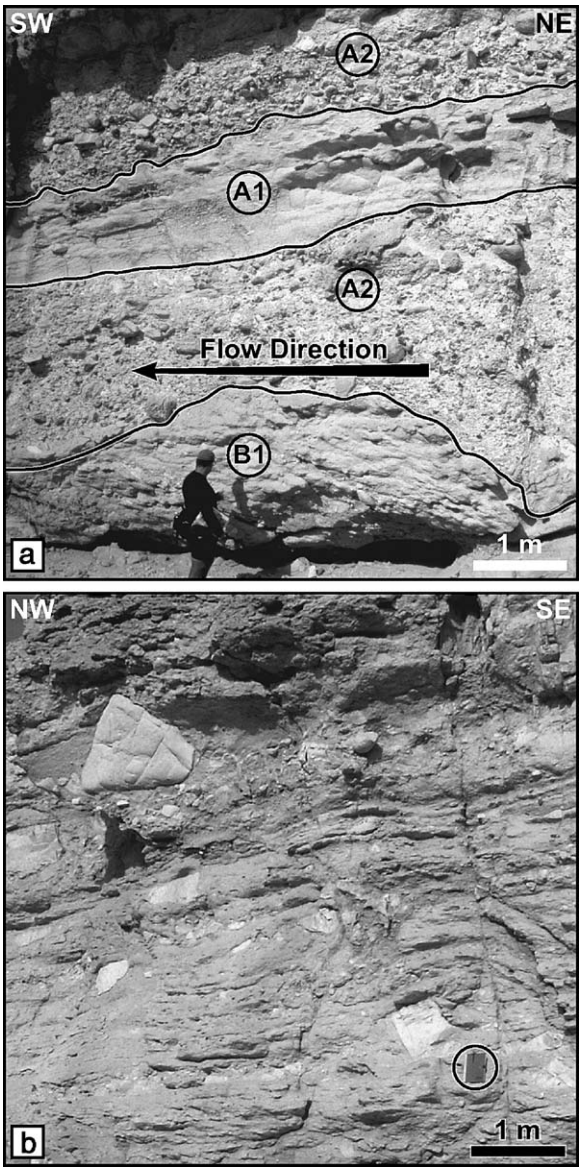

Fig. 2. (a) Characteristics of Facies Association A; erosively based, lobate cobble-grade conglomerates (Facies A2) interbedded with medium to coarse-grained bedded sandstones (Facies A1). Note slump block of Facies Association B draped by Facies A2. See Fig. 9 for location. (b) Medium to coarse-grained bedded sandstone (Facies A1) consisting of decimetre-scale beds disturbed by large sub-angular outsized pre-rift limestone lithoclasts (notebook for scale). See Fig. 9 for location.

throughout. This facies often displays a mottled texture indicating possible bioturbation, and this becomes more evident towards the top surface of the individual sheets or broad lobes. Shell hash and occasional disarticulated oysters (*Hyotissa* sp.) are present throughout. These sandstones are interbedded with Facies A2 (lobate cobble-grade conglomerate), B1 (contorted medium to coarse-grained bedded sandstone) and D1 (green laminated siltstone) and extend basinwards up to 250 m from the fault. Individual sheets or broad lobes have an along strike continuity of <500 m. Contacts with adjacent facies are typically sharp, although a gradational basal contact with the conglomerates of Facies A2 is common.

Lobate cobble-grade conglomerate (A2) consists of sub-angular to rounded, clast supported, moderately sorted conglomerates that form fining-upwards, lobate units 2 to 5 m thick. Clasts in Facies A2 range from 2 to 10 cm in diameter and consist of limestone and chert lithoclasts (Fig. 2a). This facies is unfossiliferous. These conglomerates are interbedded with Facies A1, B1 and D1 and extend for approximately 150 m basinwards from the fault. Individual lobes have an along strike continuity of <400 m. Contacts with adjacent facies are typically sharp, although a gradational upper contact with the sandstone of Facies A1 is common.

Interpretation of Facies Association A—the overall geometry and limited dip extent of individual lobes combined with the fault-parallel elongation highlight the control the Thal fault had on the development and evolution of these facies. The presence of coalescing lobes forming a linear belt indicates a multiple-source feeder system (Reading and Richards, 1994). The sub-angular nature of the clasts indicates limited reworking and short transport distances, which combined with the pre-rift source of the lithoclasts suggests the footwall scarp of the Thal fault could have been a local source for these lobes.

The coarse grain size, floating clasts, sharp erosive base and fining upwards nature of individual beds suggests transport via concentrated density flow processes (Lowe, 1982; Mulder and Alexander, 2001) and subsequent deposition from suspension due to waning flow conditions. Possible triggering mechanisms for these flows could be fault movement or other seismic activity in the area, or possibly storm events. Concentrated density flows can transport large clasts as they relay on dispersive pressure generated from grain-to-grain interaction to act as an important particle support mechanism to keep grains in suspension (Bagnold, 1954). They also allow particle fallout within the flow resulting in differential settling and sorting, i.e. fining upwards (Mulder and Alexander, 2001). Previous studies of concentrated density flows (e.g. Piper and Savoye, 1993; Mulder et al., 1997) have shown that they can be strongly erosional, the product of this erosion supplies sediment to the flow, in some cases >80% of the material recorded in the final deposit (e.g. 1979 Nice

density flow documented by Piper and Savoye, 1993; Mulder et al., 1997). The driving force behind concentrated density flows is principally gravity (Mulder and Alexander, 2001), and this combined with the composition and sub-angular nature of the deposits supports the local elevated footwall source for the flows. The shell hash, oyster fragments and organisms responsible for the possible bioturbation in Facies A1 could have been swept down into the hangingwall depositional environment by these flows from shallow water environments rimming the footwall. Facies Association A represents a linear-source slope apron (Reading and Richards, 1994) formed by the deposition of locally sourced, structurally confined, lobate, concentrated density flows in the immediate hangingwall to the Thal Fault.

3.1.2. Facies Association B: slumps and slides

Facies Association B is distinguished by soft sediment deformation and comprises one facies, contorted medium to coarse-grained bedded sandstone (B1). These contorted sandstones are pale brown, bioclastic sandstones (similar to Facies A1) crudely bedded on a 15 cm scale that form 2 to 5 m thick highly contorted sheets bound by slide planes and occur in the immediate hangingwall to the Thal Fault Zone. Internally Facies B1 is thrusted and folded in a multilayer, duplex style with a basinwards, fault perpendicular vergence towards the west. Basal contacts of individual units are sharp and result in an angular discordance between the bedding in the contorted sandstones above and the intact facies below. The upper contact of these contorted sheets is draped by the overlying facies. The slumped intervals form intraformational units with Facies Association A (Fig. 2a) and Facies D1 and extend basinwards up to 300 m from the fault. Individual sheets have an along strike continuity of <400 m.

Interpretation of Facies Association B—the internal deformation, lateral discontinuity, slide planes and intraformational relationship with slope apron deposits (Facies Association A) suggest that Facies Association B is the product of submarine landsliding of the slope apron strata. The sedimentology of Facies B1 supports this interpretation, as it is similar in character to that of the slope apron sandstones of Facies A1. The structural location of the slope apron in the immediate hangingwall to the Thal fault and the under-filled nature of the basin could have resulted in depositional lobes with high to very high slope gradients (Reading and Richards, 1994). These lobes would have been unstable and prone to failure. The slide planes and syn-depositional slump-fold structures suggest the sandstone was semi-lithified prior to slumping (Gawthorpe and Clemmey, 1985; Martinsen, 1989). This allowed the slide mass to retain its identity and fold in a multilayer style. Possible triggering mechanisms for these slumps and slides could be over-steepening of the slope gradient on the lobe, or failure caused by seismic triggering due to movement on

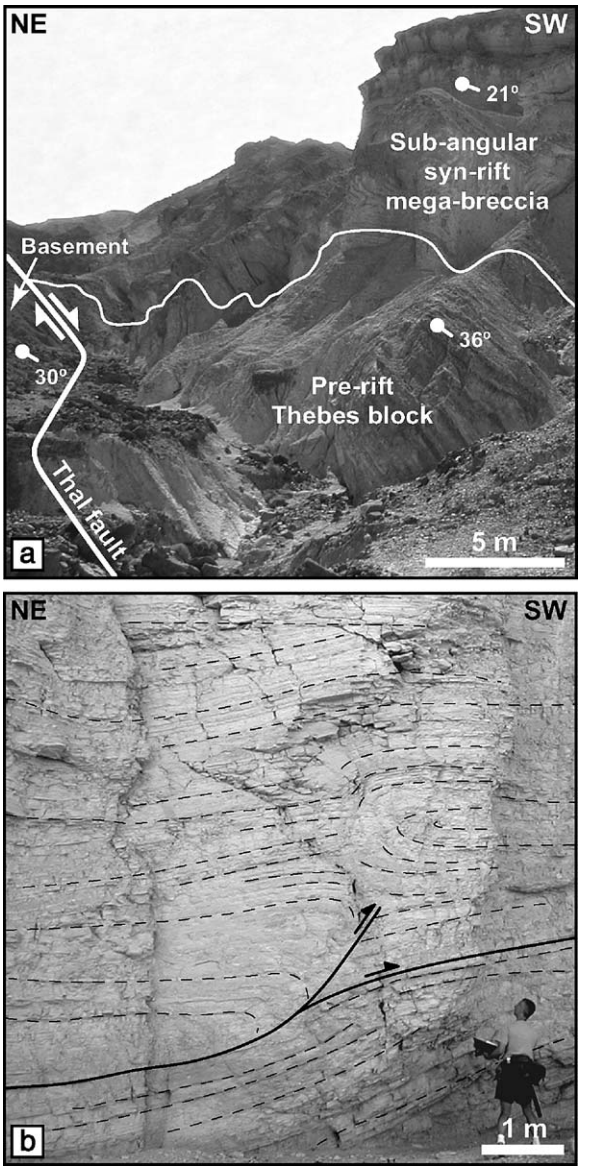

Fig. 3. (a) Facies Association C in the immediate hangingwall to the Thal fault in the Gebel Nukhul area (Fig. 1a). The large, tabular pre-rift Thebes block is at least 200 m long and is encased by the sub-angular mega-breccia of Facies C1. (b) Interbedded siltstones and fine-grained sandstones of the lower slope/basinal Facies Association D. These deposits are locally deformed, displaying syn-sedimentary, isoclinal recumbent folds and thrusts. Dashed lines highlight bedding. See Fig. 1a for location.

the Thal Fault or other faults in the area. Facies Association B represents submarine slumps and slides off the front of a slope apron in the immediate hangingwall to the Thal Fault.

3.1.3. Facies Association C: fault scarp degradation complex

Facies Association C consists of white, pebble-to-boulder-grade, clast-supported, sub-angular mega-breccia (C1) that forms deposits up to 150 m thick in the immediate hangingwall to the Thal Fault Zone, that extend for >2 km parallel to the fault (Fig. 3a). Contacts with adjacent facies are typically sharp and erosional at the base, with a gradational upper contact. Clasts in Facies C1 are predominantly limestones of the pre-rift Thebes Formation with an average clast size of 0.45 m diameter, but there are also large tabular-shaped blocks at least 200 m long (Fig. 3a). These mega-breccias form intraformational units with Facies D1. There are no body fossils or bioturbation in this facies. The mega-breccia units pinch out abruptly basinwards within 250 m of the fault scarp into siltstones of the lower slope Facies D1, although isolated blocks up to 50 m diameter can be found within the lower slope up to 300 m basinward of the fault zone. Facies Association C is restricted to the area of highest displacement on the Thal Fault Zone in the Gebel Nukhul area (Fig. 1a).

Interpretation of Facies Association C—the structural location, clast size and immature texture suggest that Facies Association C represents a fault scarp degradation complex, sourced from the pre-rift limestone in the footwall of the Thal Fault. Using the classification of Varnes (1978), Facies C1 is interpreted as a rock-fall mega-breccia, with the sub-angular shape of the clasts suggesting a short transport distance. The size (at least 200 m) and intact nature of the larger blocks present indicates that they may have slid from the footwall into the immediate hangingwall basin. The folding and basinward dip of pre-rift units in the footwall and the basinwards dip of the blocks in the hangingwall (Fig. 3a) suggests that fault propagation folding may have been a possible mechanism for this deformation (Gawthorpe et al., 1997; Sharp et al., 2000a). Weak layers in the folded pre-rift strata of the footwall may have acted as décollement surfaces for large blocks to slide basinwards into the immediate hangingwall depocentre. Similar fault-scarp degradation complexes have also been interpreted on 3D seismic data in the

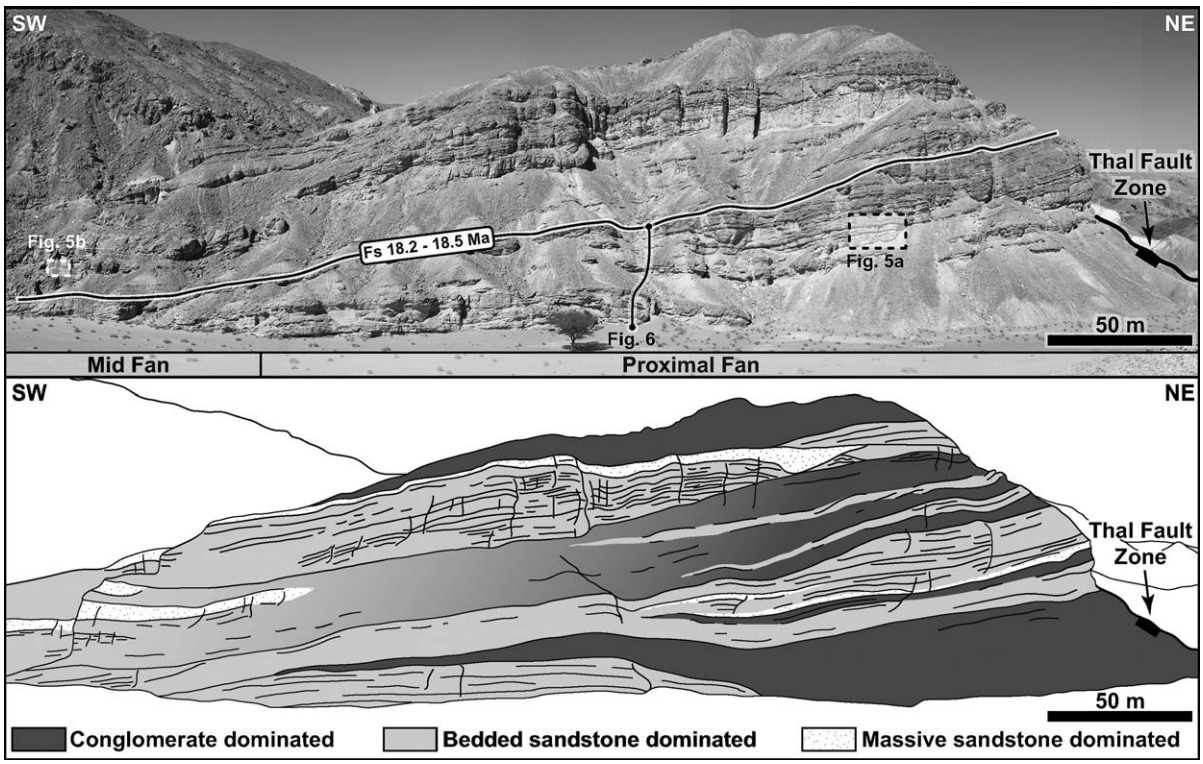

Fig. 4. Photograph and line drawing of the North face of Wadi El Hommer, Gebel Sarbut El Gamal area (Figs. 1a and 9) highlighting the facies distribution and stratigraphic architecture of the proximal fan (Facies Association E) to mid fan (Facies Association F) facies in the immediate hangingwall to the Thal fault zone.

immediate hangingwall to the Strathspey-Brent-Statfjord Fault in the North Sea rift (McLeod et al., 2002). The interpretation of the environment within which the fault scarp degradation complex was deposited is problematic due to the lack of diagnostic environmental indicators such as borings and karstic surfaces. However, the juxtaposition of Facies Association C and the lower slope facies (Facies Association D) suggests deposition in a lower slope/basinal marine environment.

3.1.4. Facies Association D: lower slope

Facies Association D comprises green laminated siltstones (D1) (70%) and siltstones to fine-grained sandstones (D2) (30%) that form units up to 20 m thick that are sheet-like, extending for >5 km along strike, >2 km basinwards. Facies Association D interfingers with the all slope and submarine fan facies. Folds and faults verge basinwards, predominantly strike fault parallel and are localized to within 800 m of the fault zone.

Green laminated siltstone (D1) consists of sheet-like units bedded on a 20 to 50 mm scale. Internally Facies D1 displays planar lamination on a 2 to 10 mm scale and contacts with adjacent facies are typically sharp (Fig. 3b). Body and trace fossils are rare, where present they include granule-grade shell hash, sand-filled *Thalassinoides* burrows up to 15 mm in diameter descending from the base of overlying sand-rich slope apron and submarine fan deposits where present. This facies can be traced basin-wide within the limits of the present day exposure.

Siltstone to fine-grained sandstone (D2) consists of grey, laminated siltstones that form laterally extensive sheet-like units bedded on a 20 to 100 mm scale (Fig. 3b). Internally Facies D2 is laminated on a 5 to 20 mm scale and displays unidirectional current ripples on the upper surface of beds, flute casts and rare mudstone rip-up clasts up to 2 mm diameter at the base of individual beds. Contacts with adjacent facies are typically sharp. Body and trace fossils are rare, where present they include shell hash and sand-filled *Thalassinoides* burrows up to 10 mm diameter descending from the base of overlying sand-rich facies.

Interpretation of Facies association D—the fine-grained nature and lamination of Facies D1 suggests deposition in a low energy environment from suspension. The siltstones and sandstones of Facies D2 exhibit classic Bouma b, c and d divisions and are interpreted to be the result of surge-like turbidity flows (Bouma, 1962; Mulder and Alexander, 2001). Bivalve shell hash was probably transported into this environment via submarine flows associated with the adjacent slope apron and submarine fan complex. The fault-perpendicular, basinward orientation of the fold and thrust structures suggests the presence of a paleoslope, perpendicular to the Thal fault zone, dipping into the hangingwall. The depositional style, spatial relationships with other facies associations and basin-wide extent of these siltstones

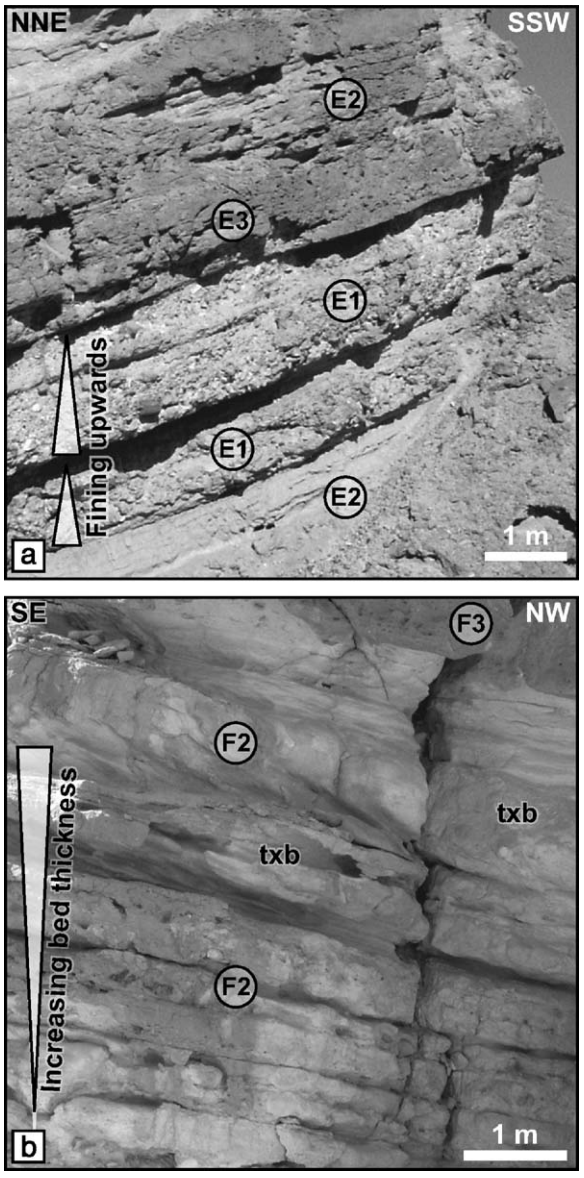

Fig. 5. (a) Interbedded lobate cobble-grade conglomerates (Facies E1), medium to coarse-grained bedded sandstone (Facies E2) and coarse-grained massive sandstones (Facies E3) of the proximal fan Facies Association E. Note the sharp base and fining upward nature of Facies E1 (see Fig. 4 for location). (b) Medium to coarse-grained upwards thickening sandstones of Facies F2 displaying low-angle bedding and metre-scale trough cross-bedding below the coarse-grained, massive sandstones of the mid fan Facies F3 (see Fig. 4 for location).

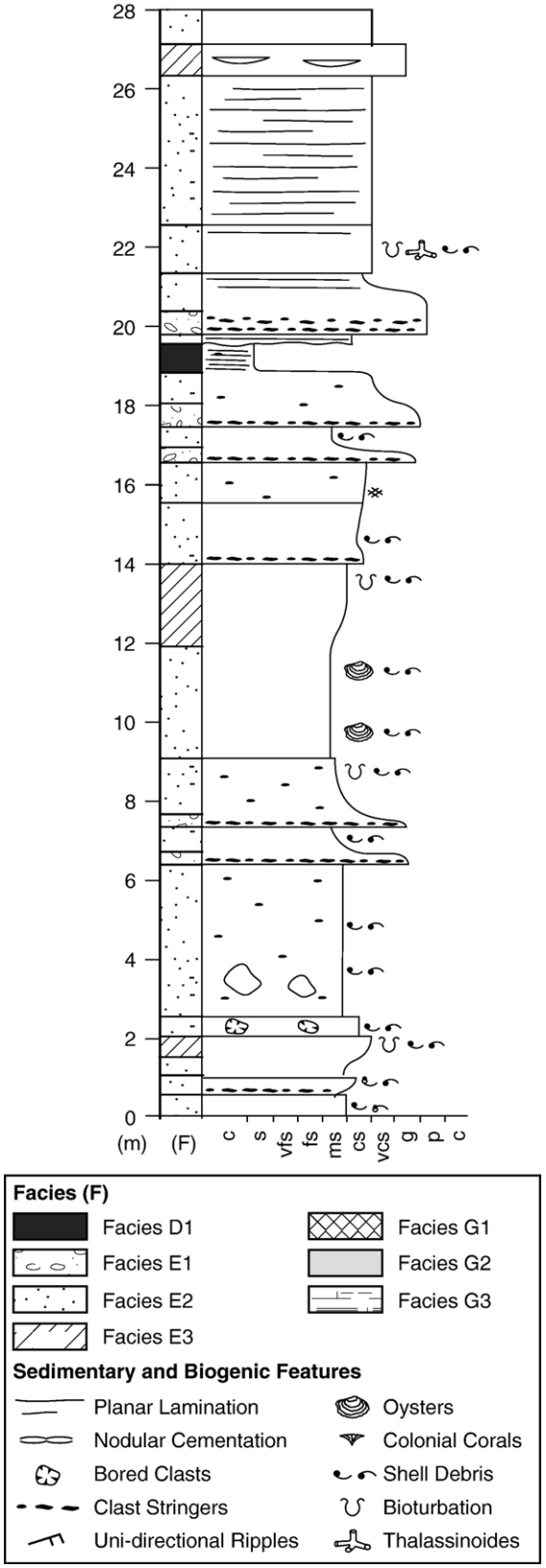

Fig. 6. Sedimentary log (measured section) through the proximal fan Facies Association E from the North face of Wadi El Hommer, Gebel Sarbut El Gamal area (see Fig. 4 for location).

and sandstones suggest that these facies were deposited in a lower slope/basinal environment.

3.2. Submarine fan complex

The three facies association of the submarine fan complex form a lobate fan system at least 130 m thick, located in the immediate hangingwall to the Thal Fault Zone. The facies associations extend laterally for >2 km, at their maximum width, and >1 km basinward.

3.2.1. Facies Association E: proximal fan

Units of Facies Association E are at least 130 m thick and consist of basinward tapering, lobate cobble conglomerates (E1) (60%) interbedded with coarse-grained, lobate, bedded sandstones (E2) (35%) and channelised massive sandstones (E3) (5%) (Fig. 4). These facies form a confined proximal fan that passes laterally into the slope apron Facies Association A along strike, and pass distally within 250–600 m of the Thal Fault Zone into the sandstone-dominated, mid fan facies of Facies Association F.

Cobble-grade conglomerate (E1) consists of erosively based, fining-upwards beds of sub-angular to rounded, clast-supported conglomerates that are moderately sorted and form basinward tapering 5 to 6 m thick units with a lobate geometry (Fig. 5a). Clasts in Facies E1 range from 10 cm to 80 cm (average 0.15 m) in size and consist of pre-rift limestone and chert (Fig. 6). This facies is unfossiliferous. Basal contacts with adjacent facies are typically sharp, although a gradational upper contact with the sandstone of Facies E2 is common. These conglomerates are interbedded with Facies E2 and E3 and extend approximately 250 m basinward from the fault and have an along-strike continuity of <1 km (Fig. 4).

Medium to coarse-grained bedded sandstone (E2) comprises poorly sorted, pale yellow, bioclastic sandstones bedded on a decimetre-scale that form lobate, basinward tapering units 5 to 6 m thick (Fig. 5a). Limestone and chert lithoclasts up to 30 mm diameter are present throughout with the occasional sub-angular limestone clast up to 60 cm diameter (Fig. 6). Basal contacts are typically sharp, although a gradational basal contact with the conglomerates of Facies E1 is common. This facies often displays a mottled texture indicating possible bioturbation, which becomes more evident

towards the top surface of the individual lobes. Shell hash and occasional disarticulated oysters (*Hyotissa* sp.) are present throughout, with algal rhodoliths present towards the top of the section. These sandstones are interbedded with Facies E1 and E3, extend for up to 250 m basinward from the fault and have a lateral continuity of <1 km (Fig. 4).

Coarse-grained massive sandstone (E3) consists of pale yellow, poorly sorted bioclastic sandstones that form 1 to 2 m thick lenses to channel-like bodies (Fig. 5a). Facies E3 is internally structureless, with outsized, floating sub-angular limestone and chert clasts up to 30 mm diameter, and commonly has a basal lag of these clasts up to 10 cm diameter (Fig. 6). Basal contacts are typically sharp and erosive, with up to 75 cm relief at the base, and display planar tops. This facies often displays a mottled texture indicating possible bioturbation. Shell hash comprised of oyster (e.g. *Hyotissa* sp.) and *Pectin* fragments along with algal rhodoliths are present throughout. These sandstones are interbedded with Facies E1 and E2 and extend for approximately 600 m basinward from the fault and along strike for <100 m (Fig. 4).

Interpretation of Facies Association E—the wedge-like geometry, sedimentology and location of these deposits suggest deposition in a marine environment immediately adjacent to a fault scarp. The limited spatial extent (<1 km along strike and up to 600 m basinward) of the cobble-grade conglomerates of Facies E1 and the medium to coarse-grained bedded sandstones of Facies E2 are comparable to the gravel-rich submarine fjord cones from British Columbia described by Prior and Bornhold (1988) and the gravel-rich submarine fan model of Reading and Richards (1994). The geometry and spatial extent of Facies Association E suggest a single point-sourced feeder system although, due to the present-day footwall erosion level, evidence of the feeder system is no longer preserved.

The character of the coarse-grained, sharp-based fining-upward, basinward-tapering, wedge-like cobble-grade conglomerate bodies of Facies E1 suggest transportation via concentrated density flow processes (Lowe, 1982; Mulder and Alexander, 2001) and deposition from suspension due to waning flow conditions. The sub-angular to rounded nature of the pre-rift limestone and chert lithoclasts present in Facies E1 and E2 highlights the erosive nature of concentrated density flows as they pass through the feeder system into the hangingwall basin. The presence of shallow-marine material (e.g. coralline debris and shell hash) indicates material transported from a shallow marine source area possibly rimming the footwall crest of the Thal Fault, or from further up the feeder system. The change in slope angle between the footwall feeder system and hanging-wall depocentre may have been sufficient to reduce the entrainment of water in the flow, leading to grain-to-grain interaction and frictional freezing, resulting in deposition of the coarse material (Mulder and Alexander, 2001). The proximity to the fault scarp and the short run-out distances of the coarser grained deposits may be attributed to the presence of a steep gradient in the feeder system. In contrast, the erosive channel-like form of the massive sandstones of Facies E3 suggests possible bypass channels depositing material further basinward.

3.2.2. Facies Association F: mid fan

Units of Facies Association F are located further basinward, and consist of pebble grade conglomerate (F1) (15%), coarse-grained bedded sandstone (F2) (70%) and coarse-grained massive sandstone (F3) (15%) that grade up-dip into Facies Association E (Fig. 4). Along strike they grade into the lower slope facies of Facies Association D and down-dip into Facies Association G within 800 m of the Thal Fault. The facies themselves are similar to those in Facies Association E with the main differences being an overall decrease in grain size and a change from predominantly basinward tapering, lobate conglomerate bodies to more sheet-like and channelised sandstones. These broad lobes/sheets are laterally extensive for >1 km along strike.

Pebble-grade conglomerate (F1) consists of 1 to 2 m thick fining-upward packages of sub-angular to rounded, clast-supported, moderately sorted, conglomerates. These fining-upward conglomerates have a sheet to lobate form, but also occasionally form a lag 25 to 40 cm thick at the base of channels cutting into Facies F2 and F3 (Fig. 4). Internally, Facies F1 contains clasts ranging from 5 to 15 cm of reef debris, pre-rift limestone and chert lithoclasts. Clast imbrication and a bed-parallel fabric defined by elongated clasts are common. Body or trace fossils are generally rare. Basal contacts with adjacent facies are typically sharp, although a gradational upper contact with the sandstone of Facies F2 is common.

Medium to coarse-grained, upward-thickening sandstone (F2) comprises light grey to white, poorly sorted bioclastic sandstones that form 1 to 5 m thick broad lobe to sheet-like units. Internally the bed thickness increases up through the unit from 10 to 60 cm. Facies F2 contains a wide range of bio- and lithoclasts up to 0.15 mm diameter, including pre-rift limestone, reef debris and floating chert lithoclasts, as well as shell hash and rhodoliths. Sedimentary structures include low-angle

bedding and metre-scale trough cross-bedding; the latter is common towards the top of individual units (Fig. 5b). This facies often displays a mottled texture indicating possible bioturbation, which becomes more evident towards the top surface of the individual lobes where *Thalassinoides* and *Skolithos* burrows cross-cut the mottled fabric. Contacts with adjacent facies are typically sharp, although a lower gradational contact with the conglomerates of Facies F1 is common. These sandstones are interbedded with Facies F1 and F3 and extend for < 1 km basinwards from the fault and have an along-strike continuity of ca. 1 km.

Coarse-grained massive sandstone (F3) consists of buff brown, poorly sorted, shelly sandstones that form 2 to 4 m thick, sheet- to lens-like units. Facies F3 is internally structureless with rare floating sub-angular limestone and chert lithoclasts up to 0.1 m diameter. Contacts with adjacent facies are typically sharp, erosive at the base and planar at the top. Body fossils include granule-grade shell hash comprised of oyster (e.g. *Hyotissa* sp.) and *Pectin* fragments, and rhodoliths. The sandstones have a highly mottled texture, suggesting a high degree of bioturbation although it is not possible to identify individual ichnotaxa. These sandstones are interbedded with Facies F1 and F2 and extend for > 1 km basinward from the Thal Fault.

Interpretation of Facies Association F—the sharp based, fining upward, lobate pebble-grade conglomerates of Facies F1 represent concentrated density flows similar to those responsible for the basinward tapering cobble-grade conglomerates of Facies E1. These flows transported coarse-grained material further basinward of the feeder system into the basin. The low-angle bedding and metre-scale trough cross-bedding of Facies F2 (Fig. 5b) is believed to represent the migration of mouth bars that formed down dip of the feeder system, beyond the channel mouths (cf. Morris et al., 1998). In contrast, the erosive channel-like form of the coarse-grained massive sandstones of Facies F3 is believed to represent bypass channels that are feeding systems further basinward. As in Facies Association E, the coralline debris, shell hash and oyster fragments are believed to have been transported into this environment from more proximal, shallow marine environments.

The up-dip relationship with Facies Association E combined with the overall decrease in grain size, and change in stratigraphic architecture from the basinward tapering conglomerate wedges of Facies Association E to the sheet-like sandstones of Facies Association F is believed to represent the down-flow transformation of the concentrated density flows identified in Facies Association E. This flow transformation is believed to be the result of flow expansion, as flows exited the feeder system into the hangingwall basin they became less confined, resulting in the progressive entrainment of fluid and/or sediment deposition. Through the process of flow expansion, fluid turbulence progressively replaced grain-to-grain interaction as the main particle-support mechanism in the flow, due to changes in sediment concentration (Mulder and Alexander, 2001). This process led to fluid turbulence acting as the main grain support mechanism at the top of the flow and the flow head (Laval et al., 1988). Such flows are regarded as transitional flows, as the whole flow does not fit within one flow-type category. The change in the particle-support mechanism resulted in the deposition of the coarser grained fraction from the flow, resulting in the basinward grading from the conglomerate-dominated facies of the proximal fan to the sandstone-dominated facies of the mid fan down-dip.

3.2.3. Facies Association G: outer fan

Units of Facies Association G are the most distal of the submarine fan depositional system and are located > 1 km basinwards from the fault zone. They grade up-dip into Facies Association E and along strike into Facies Association D. The channelised sandstones of Facies G1 (25%) form erosively based channels and channel complexes up to 20 m thick and 20 to 30 m wide (Fig. 7a, b). In contrast, Facies G2 (15%) forms laterally extensive sheet-like deposits that can be traced for more than 800 m along strike (Fig. 7a). Interbedded with these channelised and sheet-like sandstones are the thinly bedded siltstones of Facies G3 (60%) and the lower slope facies (D1) (Fig. 7a–c). The siltstones of Facies G3 are laterally continuous and can be traced for many kilometres along strike.

Coarse-grained channelised sandstone (G1) consists of pale yellow to brown, poorly sorted, medium to granule-grade, bioclastic sandstones that have channel geometries and are up to 5 m thick and 20 to 30 m wide. Internally, the units display lateral accretion surfaces, slumped margins and form fault zone-perpendicular channels or stacked channel complexes up to 20 m thick (Fig. 7b). Facies G1 contains sub-rounded clasts up to 0.1 m in diameter of heavily bored pre-rift limestone lithoclasts (70%) and reef debris (30%), together with rare chert clasts (Fig. 8). Fossils present include granule-grade shell hash comprised of oyster and *Pectin* fragments, and relatively intact *Pectin* and oyster shells (e.g. *Hyotissa* sp.), coralline debris and rhodoliths. These sandstones are interbedded with the sheet

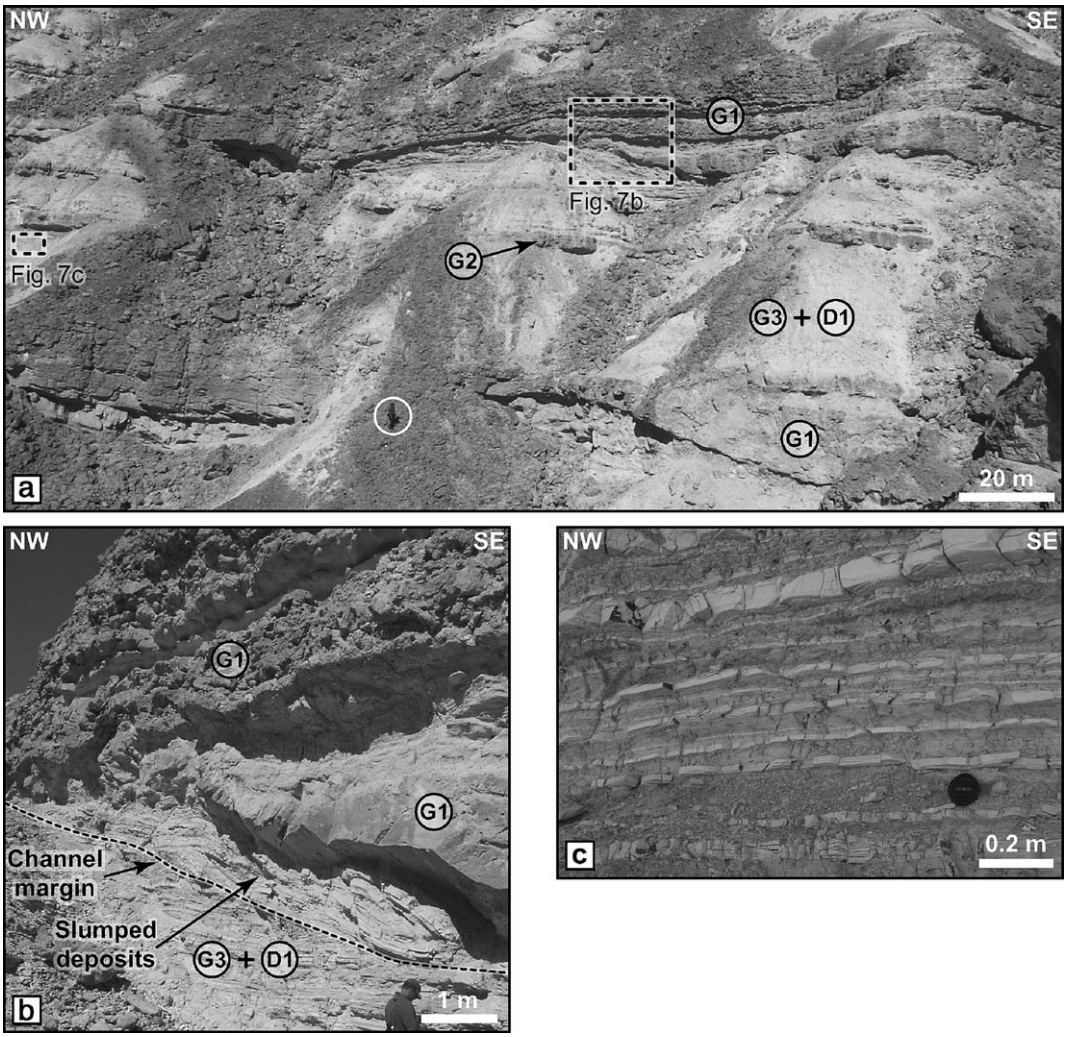

Fig. 7. (a) Photograph illustrating the relationship between the siltstone to fine-grained sheet-like deposits of distal fan Facies G3 and lower slope/basinal Facies D1, the coarse-grained channelised sandstone deposits of Facies G1, and the medium-grained sheet sandstones of Facies G2. See Fig. 9 for location. (b) Detail of the erosive contact between the channelised deposits of Facies G1 and the fine-grained sheet-like deposits of Facies G3 and D1. Note slumped facies above the channel margin. See Fig. 9 for location. (c) Interbedded siltstone to fine-grained sandstones of Facies G3 and the laminated siltstones of Facies D1. Facies G3 displays laminations on a 5 to 20 mm scale, unidirectional current ripples and rare, up to 2 mm diameter, mudstone rip-up clasts. See Fig. 9 for location.

sandstones and siltstones of Facies G2, G3 and D1 and extend for at least 1.5 km basinward from the fault zone.

Fine to medium-grained sheet sandstone (G2) comprises pale brown, bioclastic sandstones that are nodular cemented and form sheet-like units up to 3 m thick (Fig. 7a). Internally Facies G2 displays crude bedding on a decimetre-scale, highlighted by nodular weathering, and contains rare, sub-angular limestone and chert lithoclasts up to 20 mm in diameter (Fig. 8). Ichnofauna include *Diplocraterion* and *Skolithos* descending from the upper surface of the unit. Body fossils include solitary and colonial coral debris up to 20 mm in diameter, granule grade *Pectin* and oyster shell hash and rare algal rhodoliths. Contacts with adjacent facies are typically sharp and slightly erosional at the base and display planar tops.

Siltstone to fine-grained sandstone (G3) consists of grey, thinly laminated siltstones that form sheet-like beds 20 to 150 mm thick (Fig. 7c). Internally, Facies G3 is laminated on a 5 to 20 mm scale and contains unidirectional current ripples and rare, up to 2 mm diameter, mudstone rip-up clasts (Fig. 8). Body and trace fossils are rare, where present they include shell hash and sand-filled *Thalassinoides* burrows up to 10 mm in diameter that descend from the base of overlying

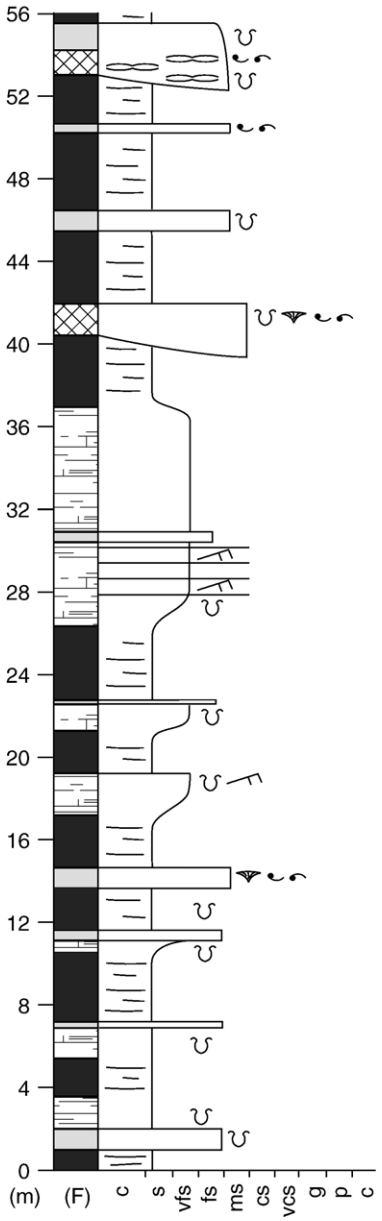

Fig. 8. Representative sedimentary log (measured section) through the distal fan Facies Association G from the east face of Gebel Sarbut El Gamal (see Fig. 1a for location). See Fig. 6 for the key to the facies and symbols used.

sand-rich facies. Contacts with adjacent facies are typically sharp.

Interpretation of Facies Association G—the channelised geometry, coarse grain size and sharp, erosively based nature of Facies G1 suggests deposition from concentrated density flow processes (Lowe, 1982; Mulder and Alexander, 2001). The presence of shallow marine material (e.g. coralline debris and shell hash) in Facies G1 indicates transport from a shallow marine source area, the hangingwall depositional location, size and sub-rounded nature of the pre-rift lithoclasts indicate they have been transported at least 1 km basinward of the inferred footwall source area. The presence of boring on all faces of these lithoclasts, however, indicates that they may have undergone multiple phases of boring, transport and deposition in a shallow marine environment. The highly erosional nature of these flows is apparent by the presence of erosional channel forms up to 5 m deep, whereas the multi-storey stacked channel fills suggest the channel was cut and then in-filled by a number of subsequent flows.

The sandstones of Facies G2 are interpreted as surge-like turbidity flows on the basis that they form sheet-like units with sharp, slightly erosive bases and planar tops, display crude bedding on a decimetre-scale and contain rare sub-angular lithoclasts and bioclasts (Mulder and Alexander, 2001). The distal location relative to other facies (e.g. Facies F3) suggests that they represent the broad terminal lobes of channel systems further up-dip. These flows probably consisted of a short flow body following the head, and were mainly depositional, producing sedimentary structures and bedforms typical of Bouma b, c and d divisions (Mulder and Alexander, 2001). Outsized bioclasts were transported by these flows due to their low density (cf. Morris et al., 1998). These surge-like turbidity flows are interpreted to be the down-dip transformation of concentrated density flows (e.g. Facies G1, F1, F2, F3). The fine-grained deposits of Facies G3 are also interpreted to be the result of surge-like turbidity flows as they exhibit the classic Bouma b, c and d divisions. These finer grained deposits are some of the most distal deposits exposed, and reflect the down-flow transformation of the concentrated density flows identified in the proximal and mid fan regions. Alternatively, they could be overbank deposits to the channelised sandstones of Facies G1.

4. Synthesis of depositional systems

Based on the characteristics of individual facies, the spatial relationships between the facies and facies associations, and their structural location in the immediate hangingwall to the Thal Fault, deposition of the Lower Rudeis Formation is interpreted to have resulted from a range of submarine concentrated density flows, surge-like turbidity flows, mass wasting and hemipelagic processes within a fault-controlled marine slope setting (Figs. 9 and 10, Table 1). Cross-sections shown in Fig. 9 are based on a series of measured sections from key localities within the hangingwall

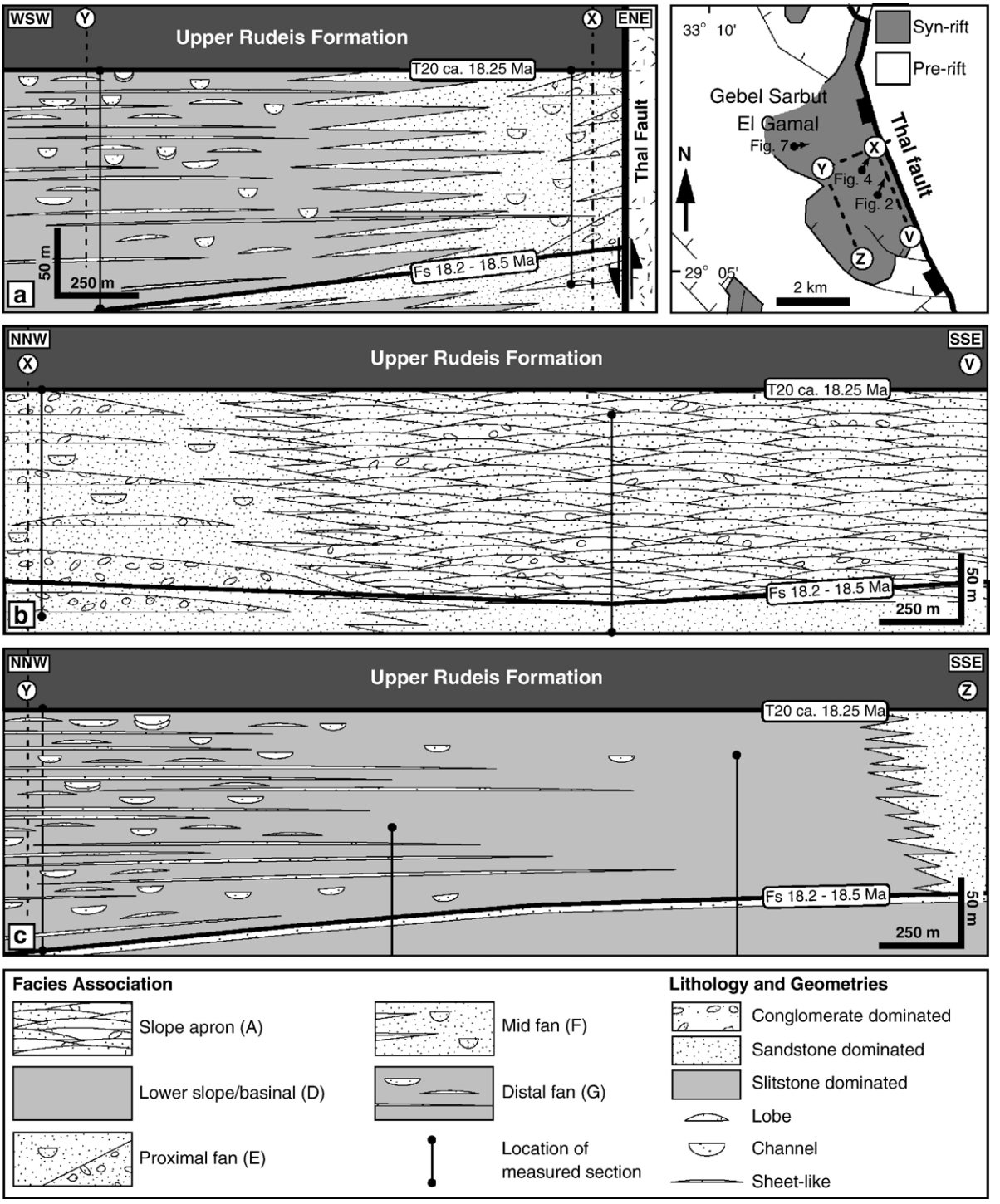

Fig. 9. Fault perpendicular (a) and fault parallel (b and c) cross-sections through the rift climax Lower Rudeis Formation in the Sarbut El Gamal segment of the Thal Fault. Sections are datumed on the mid-Rudeis unconformity (T20) surface that separates the Upper and Lower Rudeis Formations. Also note the major flooding surface (Fs; 18.2–18.5 Ma) that can be correlated basin-wide within the study area. (a) highlights the fault-perpendicular distribution of the submarine fan complex Facies Associations E, F and G. (b) highlights the fault-parallel relationship 100 m basinward of the Thal Fault between the slope apron Facies Association A and the proximal fan Facies Association E. (c) Cross-section 1.5 km basinward of the Thal Fault illustrates the fault-parallel relationship between the distal fan facies (Facies Association G) and the lower slope/basinal facies of Facies Association D.

basin. The sections are correlated at the base on a major basin-wide flooding surface (Fs, 18.2–18.5 Ma) that marks the transition from sandstone-dominated rift-initiation to mudstone-dominated rift climax deposits.

The lower slope to basinal facies of Facies Association D occur basin-wide across the Hammam Faraun Fault Block, forming laterally extensive hemipelagic siltstones and fine-grained sandstones deposited via surge-like turbidity flows in a background, low energy, lower slope to basinal environment. These surge-like turbidity flows are believed to represent the distal, down-dip transformation of the concentrated density flows identified in the slope apron and submarine fan complex facies associations. However, in proximal locations, within 250 m of the Thal Fault, the lower slope facies are overprinted by, and/or rare interbedded with, coarse-grained facies of the laterally continuous slope apron, localized submarine fan complex or fault scarp degradation facies associations (Figs. 9 and 10).

The coarse-grained concentrated density flow deposits of the slope apron (Facies Association A) form a series of small-scale lobes that coalesce to form an elongate apron confined to within 250 m of the Thal Fault (Fig. 9). Individual depositional lobes have a limited lateral extent of up to 500 m along strike, whereas the apron as a whole extends along the entire, >2 km length, of the Sarbut El Gamal Fault segment (Figs. 1a and 9). The source area for these flows is envisaged to be the adjacent footwall scarp due to the angular nature and pre-rift composition of the deposits. Down-dip, interbedded with the toes of these slope apron lobes, are localized, highly contorted intraformational sandstones bound by slide planes. These slumps and slides (Facies Association B) extend for up to 300 m basinwards of the Thal Fault and have an along-strike continuity of <400 m. The location and composition of these contorted packages suggest they are sourced directly from the slope apron deposits

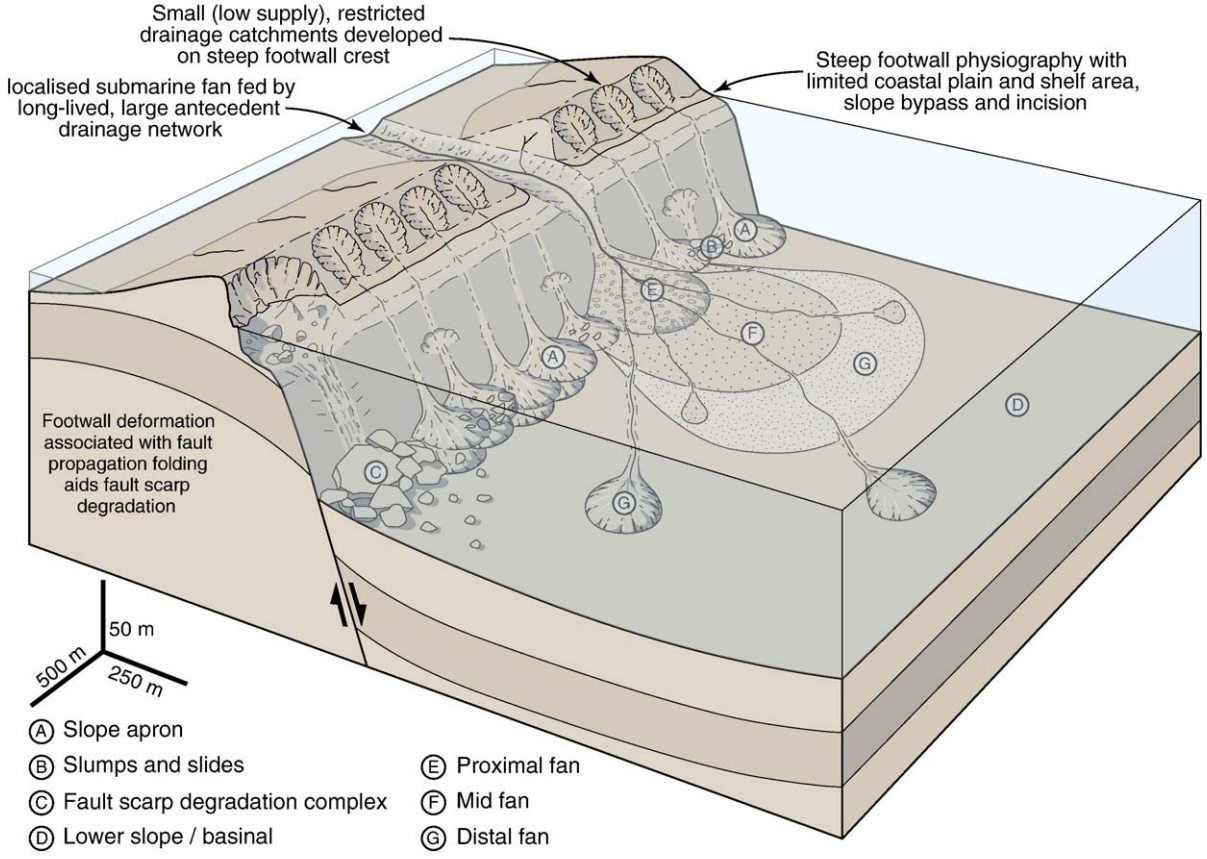

Fig. 10. Depositional model for marine rift climax deposits in the hangingwall of a major rift-bounding fault. Sediment supply is outpaced by subsidence resulting in typically deepwater, sediment-starved, hangingwall depocentres dominated by deep marine mudstones. Local development of coarser clastics is sourced in the immediate hangingwall from restricted catchments on the footwall scarp, or where fault scarp degradation complexes develop. In contrast, the localized submarine fan (Facies Association E, F and G) is interpreted to have been fed by a larger, antecedent drainage network, resulting in a point source of high sediment supply. Note, along strike variation in fault displacement and geometry not shown.

(Fig. 10). The slope apron (Facies Association A) and slump and slide deposits (Facies Association B) interfinger basinward with lower slope/basinal deposits (Facies Association D) and locally, pass laterally into the conglomerate-dominated proximal-fan region of the submarine fan complex (Facies Association E) (Fig. 9). However, in areas of present-day high fault displacement (e.g. Gebel Nukhul; Fig. 1), the immediate hangingwall deposits are characterised by large, tabular-shaped blocks up to 200 m long and breccias that represent a fault scarp degradation complex (Facies Association C) (Fig. 10).

Deposition of the localized submarine fan complex (Facies Associations E, F and G) occurred in the immediate hangingwall to the Thal fault, the facies and facies associations present reflect the mode of transport, down-flow evolution and deposition of concentrated density flows. The proximal fan comprises a stacked succession of basinwards tapering, lobate wedges of conglomerate (E1) and bedded sandstones (E2), forming bodies that are up to 1 km wide and pass along strike into the coarse-grained slope apron deposits (Figs. 4 and 9). The proximity of the coarse-grained slope apron sandstones and conglomerates to the immediate hangingwall (within 250 m of the Thal Fault) is related to the expansion of concentrated density flows as they exit the feeder channel into the hangingwall basin, become less confined and deposit coarser grained material from the flow.

The conglomerate-dominated facies of the proximal fan (Facies Association E) grade down-dip into the sandstone-dominated facies of the mid fan (Facies Association F). This transition is also marked by an overall change in geometry of the deposits from the fault confined wedges of the proximal fan to the more sheet-like/broad lobe geometries of the mid fan facies. The sheet to broad lobe-like geometries of the mid fan extend for up to 1 km basinward from the fault zone and have an along-strike continuity of ca. 1 km (Figs. 9 and 10). The change in grain size and geometry between the proximal and mid fan facies is interpreted to represent the down-flow transition of the concentrated density flows. The mid fan deposits pass along-strike into the distal remnants of the slope apron facies and, more commonly, the lower slope/basinal deposits of Facies Association D (Figs. 9 and 10). Flow transition continues basinward into the distal fan region (Facies Association G) resulting in the deposition of laterally extensive (>500 m), sheet-like, siltstone surge-like turbidity flow deposits (G3) that are interbedded with lower slope to basinal hemipelagic siltstones (D1) (Figs. 9 and 10).

Interbedded with the conglomerates and sandstones of the proximal to mid fan regions are lens-like to channelised, coarse-grained massive sandstones (E3, F3) that extend for up to 1 km basinward with an along-strike continuity of up to 500 m (Fig. 4). These coarse-grained deposits are believed to represent bypass channels that transport sediment to the solitary and stacked channel complexes (G1) observed in the distal fan (Figs. 9 and 10). These channelised sandstones (G1) are up to 30 m wide and are interpreted to represent laterally confined, concentrated density flows that have transported coarse-grained sediment over 1.5 km from the Thal Fault by maintaining a high sediment concentration, either by flow confinement or bypass. Associated with these channelised features are the sheet-like sandstones (G2) that are interpreted to represent the broad terminal lobes of the channelised sandstones of Facies G1 (Fig. 10). These broad lobes extend for >250 m along strike and at least 200 m basinward and are thought to be deposited from surge-like turbidity flows that are the down-flow transformation of the concentrated density flows that deposited the channelised sandstones of Facies G1. These surge-like turbidity flows may also have continued to run out and contributed to the deposition of the siltstones of Facies G3. The presence of the channelised sandstone of Facies G1 in this distal fan setting suggests the presence of terminal lobes further basinward than the present-day exposure.

5. Discussion

5.1. Flow transformation

In this study, subaqueous sedimentary density-flow processes are responsible for up to 60% of the facies present in the immediate hangingwall to the Thal Fault. The deposits associated with the down-flow transformation of sedimentary density flows active in the submarine fan complex (Facies Association E, F and G) can be traced basinwards over a distance of ca. 800 m from the sediment entry point into the hangingwall basin (Fig. 11). As a concentrated density flow exits the feeder system into the hangingwall basin, it becomes less confined and expands, entraining fluid into the flow and/or depositing the coarser grained material resulting in the deposition of the conglomerate-dominated, basinward-tapering wedges identified in the proximal fan Facies Association E (Fig. 11).

Through the process of flow expansion, fluid turbulence progressively replaces grain-to-grain interaction as the main particle-support mechanism due to

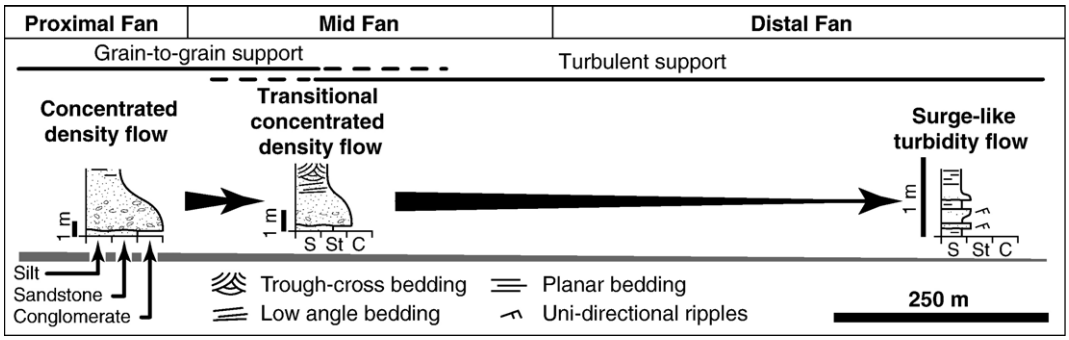

Fig. 11. Interpreted down-flow evolution of a subaqueous sedimentary density flow on the submarine fan complex in the immediate hangingwall. As the concentrated density flow exits the feeder system the flow starts to transform primarily due to flow expansion, resulting in a reduction in sediment concentration through fluid entrainment and/or deposition. As a result fluid turbulence replaces grain-to-grain interaction as the dominant particle-support mechanism (Lowe, 1982; Mulder and Alexander, 2001).

reduced sediment concentration. This results in a basinward grading of the flow deposits and a marked change in deposit geometry over a down-flow distance of ca. 250 m from the wedge-like geometries of the conglomerate-dominated proximal fan to the sheet-like geometries of the sandstone-dominated mid fan (Fig. 11). As the flow continues basinward, fluid turbulence becomes the main particle-support mechanism, resulting in a transformation to fully turbulent, surge-like turbidity flows in the distal fan some 800 m from the fault zone (Fig. 11).

Tracing of individual beds suggests that the same transport event responsible for the concentrated density flows identified in the proximal to mid fan regions may also be responsible for the surge-like turbidity flows identified in the distal fan region due to down-flow transformation (Fig. 11). Alternatively these surge-like turbidity flows may be the result of flows that have bypassed the more proximal fan regions. Bypass flows may be the result of major river flood events resulting in higher energy, higher concentration, longer run-out flows such as those observed in the Gulf of Corinth (Ferentinos et al., 1988). A similar style of down-flow transformation is also observed in the slope apron deposits, although on a much smaller scale (<200 m). The footwall scarp-derived source area for the slope apron flows results in a lower flow volume and therefore shorter run-out distance (<250 m) compared to the larger feeder system associated with the submarine fan complex.

5.2. Controls on rift climax deposition

The development of normal faults and their impact on basin physiography and slip rates exert major controls on the spatial distribution and stratigraphic architecture of depositional systems in the immediate hangingwall basin (Gawthorpe and Leeder, 2000). During rift climax, displacement is localized on a high displacement rate, through-going fault system with the development of a single large depocentre in the hangingwall of the basin bounding fault zone (Cowie et al., 2000). Fault displacement rates of 2 to 5 m ky^{-1} are typical of active normal faults and result in accommodation development generally outpacing sediment supply to the basin, creating a sediment-starved, under-filled depocentre (Gawthorpe et al., 1994; Gawthorpe and Leeder, 2000). A consequence of the under-filled nature of the hangingwall depocentre, plus the steep gradients of the normal fault, is that the basin margin physiography is steep and commonly a bypass or erosional slope, with limited coastal plain or shelf area (Papatheodorou and Ferentinos, 1993; Leeder and Jackson, 1993; Leeder et al., 2002) (Fig. 10).

The evolution of drainage networks and catchments are primary controls on sediment supply to the hangingwall basin (Allen and Densmore, 2000). Short, locally restricted drainage catchments characterise the steep, uplifted footwall scarp. Modern examples of restricted, footwall scarp drainage systems developed in a limestone bedrock lithology similar to the Suez Rift occur in the Gerania Range, Alkyonides Gulf, Greece. In this modern analogue, small, regularly spaced, elongate drainage catchments occur on steep footwall scarp slopes (mean slope, 12–22°), and these supply sediment to small fans, producing elongate slope aprons (Leeder et al., 2002). We interpret the footwall physiography of the Thal Fault during Miocene rift climax times to have been similar, with low sediment supply and high hangingwall subsidence rates leading to the development of a narrow fringe of slope apron deposits (Facies Association A) confined to the

immediate hangingwall basin. Elongate rift climax deposits, confined to the immediate hangingwall, are a common feature in many extensional marine basins, e.g. East Greenland rift (Surlyk, 1989), Barents Sea (Prosser, 1993), East Shetland basin (McLeod et al., 2002), Gulf of Corinth (Gawthorpe and Leeder, 2000) (Fig. 10).

In contrast to the restricted footwall drainage systems, antecedent drainage systems with large catchments and high sediment discharge are believed to control the location of the point-sourced major submarine fan complex (Facies Associations E, F and G) in the centre of the Sarbut El Gamal segment (Figs. 1, 4 and 10). This drainage system is interpreted to be similar to modern examples from the footwall of the active Gulf of Corinth rift (e.g. Akrata and Xylokastro Deltas (Seger and Alexander, 1993) where incision has kept pace with footwall uplift and sediment transport is maintained into the hangingwall depocentre. Transfer zones associated with lower overall fault displacement at major segment boundaries also develop aerially extensive drainage networks that may act as sites of localized coarse clastic sediment input into the hangingwall basin (e.g. Young et al., 2002).

In the study area, another control on the development of depositional systems and syn-rift stratigraphy is the bedrock lithology and structure in the footwall source area. The unroofing history of the pre-rift stratigraphy in the restricted footwall scarp catchments has a direct influence on the deposits in the immediate hangingwall. The erosion of a mudstone-dominated pre-rift unit in the footwall (e.g. the shale-dominated, Paleocene Esna Formation) provides only fine-grained sediment to the hangingwall depocentre. Thus once the Eocene Thebes Formation is unroofed, and the Paleocene Esna Formation exposed, there is an apparent major shutdown of coarse-clastic deposition, manifested by widespread mudstone deposition in the immediate hangingwall. Without knowledge of the pre-rift source area lithology, the abrupt change to mudstone deposition may be incorrectly interpreted to result from an abrupt increase in relative sea level. The steep physiography of the footwall scarp combined with the deformation associated with fault propagation folding in the footwall (Gawthorpe et al., 1997; Sharp et al., 2000a) is interpreted to influence slope bypass through the development of fault-scarp degradation complexes. Basinward-dipping bedding planes in the uplifted footwall scarp act as décollement surfaces on which large pre-rift blocks detach and slide into the immediate hangingwall basin (Figs. 3a and 10). This fault propagation folding structural style is believed to be a primary control on slope bypass in fault segments with the highest present-day displacement, resulting in the highest scarps, with the steepest slope gradient and deepest hangingwall basin (e.g. the Gebel Nukhul segment of the Thal Fault; Figs. 1 and 3a).

6. Conclusions

The Lower Rudeis Formation in the immediate hangingwall to the Thal Fault can be divided into two contemporaneous depositional systems: (i) a laterally continuous slope system, comprising a slope apron, slumps and slides, fault scarp degradation complex, and lower slope to basinal deposits, and (ii) a localized submarine fan complex comprising proximal fan conglomerates, mid fan sandstones, and distal fan sandstones and mudstones. The scale and restricted areal distribution of these facies and facies associations reflects the low sediment supply and high accommodation setting in the immediate hangingwall of a major normal fault. The facies, facies relationships and spatial variability documented in the immediate hangingwall to the Thal Fault indicate that deposition occurred via a range of submarine, concentrated density flows, surge-like turbidity flows, mass wasting and hemipelagic processes.

The coarse-grained slope apron facies form a narrow, <250 m wide, laterally extensive apron comprising small-scale lobes sourced from the immediate footwall scarp that were deposited from concentrated density flows. Interbedded with the toes of the slope apron are highly contorted, slumped deposits sourced directly from the slope. Basinward, and interbedded with toes of these deformed units are the lower slope to basinal facies that form laterally extensive interbedded hemipelagic and fine-grained, surge-like turbidity deposits. However, in areas of high fault displacement, deposits in the immediate hangingwall are characterised by fault scarp degradation complexes comprising of large tabular blocks at least 200 m long encased in a sub-angular mega-breccia that pinch-out into lower slope to basinal facies within 250 m of the immediate hangingwall.

In contrast to the laterally extensive slope apron, a submarine fan complex is restricted to a ca. 2 km wide zone in the immediate hangingwall at the centre of the Sarbut El Gamal Fault segment of the Thal Fault. The fan complex comprises of a conglomerate-dominated proximal fan up to 1 km wide that passes down-dip within 250 m into the sandstone-dominated mid fan region, which in turn passes down-dip within 800 m of the Thal Fault into the fine-grained, sandstone-dominated distal fan that extends at least 1.5 km basinward of the Thal Fault. The deposits of the submarine fan

complex reflect down-flow evolution from concentrated density flows to surge-like turbidity flows.

Major controls on the spatial variability and stratigraphic architecture of the depositional systems reflect the physiography, accommodation and drainage evolution associated with the growth of the Thal Fault. High fault displacement rates generally result in accommodation development outpacing sediment supply to the basin, resulting in a sediment-starved basin. The underfilled nature of the hangingwall depocentre, combined with the steep gradients of the normal fault, results in a basin margin with a steep physiography and limited coastal plain or shelf area that was characterised by slope bypass or erosion. The limited basinward extent and along-strike elongation of the slope apron deposits in the immediate hangingwall is a direct reflection of the numerous, small, restricted drainage catchments on the steep footwall crest. In contrast, the localized submarine fan is interpreted to have been fed by long-lived, relatively large antecedent drainage networks.

Bedrock lithology and the structure of the immediate footwall also exert a control on facies development and stratigraphic evolution. The unroofing history of the pre-rift stratigraphy has a direct influence on the deposits in the immediate hangingwall, particularly when different formations erode to provide contrasting sediment grain size populations. In areas of high fault displacement, fault scarp degradation exploits the steep footwall physiography and basinward-dipping bedding in pre-rift footwall strata associated with fault-propagation folding.

Acknowledgments

This work was funded by NERC (Grants GR3112947 to RLG and NER/S/J/2000/04064to CWL) with additional financial support from BP Egypt/GUPCO. The authors gratefully acknowledge BP Egypt, GUPCO, EGPC, Sayeed and Gamal Gouda for logistical support in the field. Ernesto Abbate and an anonymous reviewer are thanked for critical reviews, which improved the manuscript. Christopher A.-L. Jackson is thanked for help and discussions in the field.

References

Abul-Nasr, R.A., 1990. Re-evaluation of the Upper Eocene rock units in west central Sinai, Egypt. M.E.R.C. Ain Shams University. Earth Science Series, vol. 4, pp. 234–247.

Abul-Nasr, R.A., 1992. Palaeoecology and sedimentary environments of Middle-Upper Eocene rocks in west central Sinai, Egypt. M.E.R.C. Ain Shams University. Earth Science Series, vol. 6, pp. 126–138.

Abul-Nasr, R.A.A., Thunell, R.C., 1987. Eocene eustatic sea level changes, evidence from western Sinai, Egypt. Palaeogeography, Palaeoclimatology, Palaeoecology 58, 1–9.

Allen, P.A, Densmore, A.L., 2000. Sediment flux from an uplifting fault block. Basin Research 12 (3–4), 367–380.

Bagnold, R.A., 1954. Experiments on a gravity-free dispersion of large solid spheres in a Newtonian fluid under shear. Proceedings of the Royal Society of London. Series A, Mathematical and Physical Sciences 225 (1160), 49–63.

Bentham, P.A., Wescott, W.A., Krebs, W.H., Lund, S.P., 1996. Magnetostratigraphic correlation and dating of the Early to Middle Miocene stratigraphy within the Suez Rift. American Association of Petroleum Geologists Bulletin 79, 1197–1198.

Bosworth, W., 1985. Geometry of propagating continental rifts. Geology 316, 625–628.

Bouma, A.H., 1962. Sedimentology of Some Flysch Deposits: A Graphic Approach to Facies Interpretation. Elservier, Amsterdam. 168 pp.

Colletta, B., Le Quellec, P., Letouzey, J., Moretti, I., 1988. Longitudinal evolution of the Suez Rift structure (Egypt). Tectonophysics 153 (1–4), 221–233.

Cowie, P.A., Gupta, S., Dawers, H., 2000. Implications of fault array evolution for syn-rift depocentre development: insights from a numerical fault growth model. Basin Research 12 (3–4), 241–261.

Evans, A.L., 1988. Neogene tectonic and stratigraphic events in the Gulf of Suez area, Egypt. Tectonophysics 153, 235–247.

Ferentinos, G., Papatheodorou, G., Collins, M.B., 1988. Sediment transport Processes on an active submarine fault escarpment: Gulf of Corinth, Greece. Marine Geology 83 (1–4), 43–61.

Garfunkel, Z., Bartov, Y., 1977. Tectonics of the Suez Rift. Geological Survey of Israel, Bulletin 71, 1–41.

Gawthorpe, R.L., Clemmey, H., 1985. Geometry of submarine slides in the Bowland basin (Dinantian) and their relation to debris flows. Journal of the Geological Society 142, 555–565.

Gawthorpe, R.L., Hurst, J.M., 1993. Transfer zones in extensional basins—their structural style and influence on drainage development and stratigraphy. Journal of the Geological Society 150, 1137–1152.

Gawthorpe, R.L., Leeder, M.R., 2000. Tectono-sedimentary evolution of active extensional basins. Basin Research 12 (3–4), 195–218.

Gawthorpe, R.L., Fraser, A.J., Collier, R.E.L., 1994. Sequence stratigraphy in active extensional basins—implications for the interpretation of ancient basin-fills. Marine and Petroleum Geology 11 (6), 642–658.

Gawthorpe, R.L., Sharp, I.R., Underhill, J.R., Gupta, S., 1997. Linked sequence stratigraphic and structural evolution of propagating normal faults. Geology 25, 795–798.

Gawthorpe, R.L., Jackson, C.A.L., Young, M.J., Sharp, I.R., Moustafa, A.R., Leppard, C.W., 2003. Fault growth, interaction, linkage and death: evolution of the Hammam Faraun fault block, Suez Rift, Egypt. Journal of Structural Geology 25, 883–895.

Gupta, S., Cowie, P.A., Dawers, N.H., Underhill, J.R., 1998. A mechanism to explain rift-basin subsidence and stratigraphic patterns through fault-array evolution. Geology 26 (7), 595–598.

Jackson, C.A.L., Gawthorpe, R.L., Sharp, I.R., 2002. Growth and linkage of the East Tanka fault zone, Suez rift: structural style and syn-rift stratigraphic response. Journal of the Geological Society 159, 175–187.

Jackson, C.A.L., Gawthorpe, R.L., Leppard, C.W., Sharp, I.R., 2005. Rift-initiation development of normal fault blocks: insights from the Hammam Faraun fault block, Suez Rift, Egypt. Journal of the Geological Society 162, 1–19.

Krebs, W.N., Wescott, W.A., Nummedal, D., Gaafar, I., Azazi, G., Karamat, S., 1997. Graphic correlation and sequence stratigraphy of Neogene rocks in the Gulf of Suez. Bulletin of the Geological Society of France 168, 63–71.

Laval, A., Cremer, M., Beghin, P., Ravenne, C., 1988. Density surges: two dimensional experiments. Sedimentology 35, 73–84.

Leeder, M.R., Jackson, J.A., 1993. The interaction between normal faulting and drainage in active extensional basins, with examples from the western United States and central Greece. Basin Research 5 (2), 79–102.

Leeder, M.R., Collier, R.E.Ll., Aziz, A.L.H., Trout, M., Ferentinos, G., Papatheodorou, G., Lyberis, E., 2002. Tectono-sedimentary processes along an active marine/lacustrine half-graben margin: Alkyonides gulf, E. Gulf of Corinth, Greece. Basin Research 14 (1), 25–41.

Lowe, D.R., 1982. Sediment gravity flows (2) depositional models with special reference to the deposits of high-density turbidity currents. Journal of Sedimentary Petrology 52 (1), 279–298.

Martinsen, O.J., 1989. Styles of soft sediment deformation on a Namurian (Carboniferous) delta slope, western Irish Namurian Basin, Ireland. In: Whateley, M.K.G., Pickering, K.T. (Eds.), Deltas: Sites and Traps for Fossil Fuels. Geological Society, London, Special Publication, vol. 41, pp. 167–177.

McLeod, A.E., Underhill, J.R., Davies, S.J., Dawers, N.H., 2002. The influence of fault array evolution on synrift sedimentation patterns: controls on deposition in the Strathspey-Brent-Statfjord half graben, northern North Sea. AAPG Bulletin 86 (6), 1061–1093.

Morris, S.A., Kenyon, N.H., Limonov, A.F., Alexander, J., 1998. Downstream changes of large-scale bedforms in turbidites around the Valencia Channel Mouth, Northwest Mediterranean: implications for paleoflow reconstruction. Sedimentology 45, 365–377.

Moustafa, A.R., 1993. Structural characteristics and tectonic evolution of the east-margin blocks of the Suez rift. Tectonophysics 223, 299–381.

Moustafa, A.R., 1996a. Structural setting and tectonic evolution of the northern Hammam Faraun block (Wadi Wasit Wadi Wardan area), eastern side of the Suez rift. Journal of the University of Kuwait-Science 23 (1), 105–132.

Moustafa, A.R., 1996b. Internal structure and deformation of an accommodation zone in the northern part of the Suez rift. Journal of Structural Geology 18 (1), 93–107.

Moustafa, A.R., Abdeen, M.M., 1992. Structural setting of the Hammam Faraun block, eastern side of the Suez Rift. Journal of the University of Kuwait-Science 19 (2), 291–309.

Mulder, T., Alexander, J., 2001. The physical character of subaqueous sedimentary density flows and their deposits. Sedimentology 48 (2), 269–299.

Mulder, T., Savoye, B., Syvitski, J.P.M., 1997. Numerical modeling of a mid-sized gravity flow: the 1979 nice turbidity current (dynamics, processes, sediment budget and seafloor impact). Sedimentology 44 (6), 305–326.

Papatheodorou, G., Ferentinos, G., 1993. Sedimentation processes and basin-filling depositional architecture in an active asymmetric graben: Strava graben, Gulf of Corinth, Greece. Basin Research 5, 235–253.

Patton, T.L., Moustafa, A.R., Nelson, R.A., Abdine, S.A., 1994. Tectonic evolution and structural setting of the Suez Rift. In: Landon, S.M. (Ed.), Interior Rift Basins. American Association Petroleum Geologists Memoir, vol. 59, pp. 7–55.

Piper, D.J.W., Savoye, B., 1993. Processes of Late Quaternary turbidity-current flow and deposition on the Var deep-sea fan, north-west Mediterranean sea. Sedimentology 40 (3), 557–582.

Prior, D.B., Bornhold, B.D., 1988. Submarine morphology and processes of fjord fan deltas and related high-gradient systems: modern examples from British Columbia. In: Nemec, W., Steel, R. J. (Eds.), Fan Deltas: Sedimentology and Tectonic Setting. Blackie, pp. 125–143.

Prosser, S., 1993. Rift-related depositional systems and their seismic expression. In: Williams, G.D., Dobb, A. (Eds.), Tectonics and Seismic Sequence Stratigraphy. Geological Society, London, Special Publication, vol. 71, pp. 35–66.

Reading, H.G., Richards, M., 1994. Turbidite systems in deep-water basin margins classified by grain-size and feeder system. AAPG Bulletin-American Association of Petroleum Geologists 78 (5), 792–822.

Refaat, A.A., Imam, M.M., 1999. The Tayiba Red Beds: transitional marine-continental deposits in the precursor Suez Rift, Sinai, Egypt. Journal African Earth Science 28, 487–506.

Seger, M.J., Alexander, J., 1993. Distribution of Plio-Pleistocene and Modern coarse-grained deltas south of the Gulf of Corinth, Greece. In: Frostick, L., Steel, R. (Eds.), Tectonic Controls and Signatures in Sedimentary Successions. International Association of Sedimentologists, Special Publication, vol. 20, pp. 37–48.

Seidler, L., Steel, R.J., Stemmerik, L., Surlyk, F., 2004. North Atlantic marine rifting in the Early Triassic: new evidence from East Greenland. Journal of the Geological Society 161, 583–592.

Sharp, I.R., Gawthorpe, R.L., Underhill, J.R., Gupta, S., 2000a. Fault propagation folding in extensional settings: examples of structural style and syn-rift sedimentary response from the Suez rift, Sinai, Egypt. Geological Society of America Bulletin 112, 1877–1899.

Sharp, I.R., Gawthorpe, R.L., Armstrong, B., Underhill, J.R., 2000b. Propagation history and passive rotation of mesoscale normal faults: implications for syn-rift stratigraphic development. Basin Research 12, 285–306.

Smale, J.L., Thunell, R.C., Schamel, S., 1988. Sedimentological evidence for early Miocene fault reactivation in the Gulf of Suez. Geology 16, 113–116.

Surlyk, F., 1989. Mid-Mesozoic syn-rift turbidite systems: controls and predictions. In: Collinson, J.D. (Ed.), Correlation in Hydrocarbon Exploration. Norwegian Petroleum Society, pp. 231–241.

Varnes, D.J., 1978. Slope movements and types and processes. In: Eckel, E.B. (Ed.), Landslides and Engineering Practice. Highway Research Board Special Report, vol. 29, pp. 20–47.

Wescott, W.A., Krebs, W.N., Dolson, J.C., Karamat, S.A., Nummedal, D., 1996. Rift basin sequence stratigraphy; some examples from the Gulf of Suez. GeoArabia 1, 343–358.

Young, M.J., Gawthorpe, R.L., Sharp, I.R., 2002. Architecture and evolution of syn-rift clastic depositional systems towards the tip of a major fault segment, Suez rift, Egypt. Basin Research 14 (1), 1–23.